

Manuscript Number: jbmt14835R1

Title: Mechanisms of cellular uptake and intracellular trafficking with chitosan/DNA/poly( $\gamma$ -glutamic acid) complexes as a gene delivery vector

Article Type: FLA Original Research

Section/Category: Biomaterials & Gene Transfer

Keywords: lysosome; macropinocytosis; caveolae-mediated pathway; transfection efficiency; cellular uptake

Corresponding Author: Dr. Hsing-Wen Sung,

Corresponding Author's Institution: National Tsing Hua University

First Author: Shu-Fen Peng

Order of Authors: Shu-Fen Peng; Michael T Tseng; Yi-Cheng Ho; Ming-Cheng Wei; Zi-Xian Liao; Hsing-Wen Sung

Abstract: Chitosan (CS)-based complexes have been considered as a vector for DNA delivery; nonetheless, their transfection efficiency is relatively low. An approach by incorporating poly( $\gamma$ -glutamic acid) ( $\gamma$ -PGA) in CS/DNA complexes was developed in our previous study to enhance their gene expression level; however, the detailed mechanisms remain to be understood. The study was designed to investigate the mechanisms in cellular uptake and intracellular trafficking of CS/DNA/ $\gamma$ -PGA complexes. The results of our molecular dynamic simulations suggest that after forming complexes with CS,  $\gamma$ -PGA displays a free  $\gamma$ -glutamic acid in its N-terminal end and thus may be recognized by  $\gamma$ -glutamyl transpeptidase in the cell membrane, resulting in a significant increase in their cellular uptake. In the endocytosis inhibition study, we found that the internalization of CS/DNA complexes took place via macropinocytosis and caveolae-mediated pathway; by incorporating  $\gamma$ -PGA in complexes, both uptake pathways were further enhanced but the caveolae-mediated pathway played a major role. TEM was used to gain directly understanding of the internalization mechanism of test complexes and confirmed our findings obtained in the inhibition experiments. After internalization, a less percentage of co-localization of CS/DNA/ $\gamma$ -PGA complexes with lysosomes was observed when compared with their CS/DNA counterparts. A greater cellular uptake together with a less entry into lysosomes might thus explain the promotion of transfection efficiency of CS/DNA/ $\gamma$ -PGA complexes. Knowledge of these mechanisms involving CS-based complexes containing  $\gamma$ -PGA is critical for the development of an efficient vector for DNA transfection.

## AUTHOR DECLARATION

We the undersigned declare that this manuscript is original, has not been published before and is not currently being considered for publication elsewhere.

We wish to draw the attention of the Editor to the following facts which may be considered as potential conflicts of interest and to significant financial contributions to this work. [OR]

We wish to confirm that there are no known conflicts of interest associated with this publication and there has been no significant financial support for this work that could have influenced its outcome.

We confirm that the manuscript has been read and approved by all named authors and that there are no other persons who satisfied the criteria for authorship but are not listed. We further confirm that the order of authors listed in the manuscript has been approved by all of us.

We confirm that we have given due consideration to the protection of intellectual property associated with this work and that there are no impediments to publication, including the timing of publication, with respect to intellectual property. In so doing we confirm that we have followed the regulations of our institutions concerning intellectual property.

We understand that the Corresponding Author is the sole contact for the Editorial process (including Editorial Manager and direct communications with the office). He/she is responsible for communicating with the other authors about progress, submissions of revisions and final approval of proofs. We confirm that we have provided a current, correct email address which is accessible by the Corresponding Author and which has been configured to accept email from [biomaterials@online.be](mailto:biomaterials@online.be).

[LIST AUTHORS AND DATED SIGNATURES ALONGSIDE]

**Shu-Fen Peng**

*Shu-Fen Peng*

**Michael T. Tseng**

*Michael T. Tseng*

**Yi-Cheng Ho**

*Yi-Cheng Ho*

**Ming-Cheng Wei**

*Ming-Cheng Wei*

**Zi-Xian Liao**

*Zi-Xian Liao*

**Hsing-Wen Sung**

*Hsing Wen Sung*

*2/30/2010*

August 26, 2010

Professor D.F. Williams, F.R. Eng.  
Editor-in-Chief  
Biomaterials

**RE: jbmt14835 Revision**

Dear Professor Williams:

Thank you very much for arranging the review process for our manuscript, jbmt14835. As suggested, the title of this manuscript has been re-organized as “Mechanisms of cellular uptake and intracellular trafficking with chitosan/DNA/poly( $\gamma$ -glutamic acid) complexes as a gene delivery vector”. Thanks again.

Sincerely yours,

Hsing-Wen Sung, Ph.D.  
Deputy Dean, R&D Office  
Tsing Hua Chair Professor  
Department of Chemical Engineering  
National Tsing Hua University  
Hsinchu, Taiwan 30013  
Phone: +886-3-574-2540  
Fax: +886-3-572-6832  
E-mail: [hwsung@che.nthu.edu.tw](mailto:hwsung@che.nthu.edu.tw)



1 **Abstract**

2 Chitosan (CS)-based complexes have been considered as a vector for DNA delivery;  
3 nonetheless, their transfection efficiency is relatively low. An approach by incorporating  
4 poly( $\gamma$ -glutamic acid) ( $\gamma$ -PGA) in CS/DNA complexes was developed in our previous study  
5 to enhance their gene expression level; however, the detailed mechanisms remain to be  
6 understood. The study was designed to investigate the mechanisms in cellular uptake and  
7 intracellular trafficking of CS/DNA/ $\gamma$ -PGA complexes. The results of our molecular  
8 dynamic simulations suggest that after forming complexes with CS,  $\gamma$ -PGA displays a free  
9  $\gamma$ -glutamic acid in its N-terminal end and thus may be recognized by  $\gamma$ -glutamyl  
10 transpeptidase in the cell membrane, resulting in a significant increase in their cellular  
11 uptake. In the endocytosis inhibition study, we found that the internalization of CS/DNA  
12 complexes took place via macropinocytosis and caveolae-mediated pathway; by  
13 incorporating  $\gamma$ -PGA in complexes, both uptake pathways were further enhanced but the  
14 caveolae-mediated pathway played a major role. TEM was used to gain directly  
15 understanding of the internalization mechanism of test complexes and confirmed our  
16 findings obtained in the inhibition experiments. After internalization, a less percentage of  
17 co-localization of CS/DNA/ $\gamma$ -PGA complexes with lysosomes was observed when compared  
18 with their CS/DNA counterparts. A greater cellular uptake together with a less entry into  
19 lysosomes might thus explain the promotion of transfection efficiency of CS/DNA/ $\gamma$ -PGA  
20 complexes. Knowledge of these mechanisms involving CS-based complexes containing  
21  $\gamma$ -PGA is critical for the development of an efficient vector for DNA transfection.  
22  
23  
24  
25  
26  
27  
28  
29  
30  
31  
32  
33  
34  
35  
36  
37  
38  
39  
40  
41  
42  
43  
44  
45  
46

47 **Keywords:** lysosome; macropinocytosis; caveolae-mediated pathway; transfection  
48 efficiency; cellular uptake  
49  
50  
51  
52  
53  
54  
55  
56  
57  
58  
59  
60  
61  
62  
63  
64  
65

## 1. Introduction

Chitosan (CS), a cationic polysaccharide, is biodegradable, non-toxic and tissue compatible [1,2]. It has the potential to condense anionic DNA into a compact structure (CS/DNA complexes) through electrostatic interactions and has been considered as a non-viral vector for gene delivery [3,4]. Although advantageous for DNA packing and protection, CS-based complexes may lead to difficulties in DNA release once arriving at the site of action intracellularly, thus limiting their transfection efficiency. To overcome this problem, an approach that can modify the internal structure of CS/DNA complexes by incorporating a negatively charged poly( $\gamma$ -glutamic acid) ( $\gamma$ -PGA) was developed in our previous study [5].

Analysis of the internal structure of CS/DNA/ $\gamma$ -PGA complexes by small angle X-ray scattering (SAXS) revealed that CS formed complexes with DNA and  $\gamma$ -PGA separately and yielded two types of domains, leading to the formation of “compounded nanoparticles” [5]. With this unique internal structure, the compounded nanoparticles might disintegrate into a number of even smaller subparticles after cellular internalization, thus improving the dissociation capacity of CS and DNA and enhancing the efficacy of gene expression [5]. In addition to improving the release of DNA intracellularly, the incorporation of  $\gamma$ -PGA in CS/DNA complexes markedly increased their cellular uptake. Similar observations were also reported by Kurosaki *et al.* [6], using cationic complexes coated with  $\gamma$ -PGA. However, the detailed mechanisms in endocytosis and intracellular routing of complexes incorporating with  $\gamma$ -PGA remain to be understood. Understanding the role of test complexes on their cellular uptake and intracellular fate is essential for the rational design of non-viral delivery devices.

The study was therefore designed to investigate the potential internalization mechanism of CS/DNA complexes with or without the incorporation of  $\gamma$ -PGA, using transmission electron microscopy (TEM) and the inhibitors specific to various endocytotic pathways. The role that  $\gamma$ -PGA may play in the cellular uptake of test complexes was modeling by molecular dynamic (MD) simulations. The intracellular routing of test complexes was

1 observed by a confocal laser scanning microscope (CLSM). Additionally, test complexes  
2 were characterized using dynamic light scattering (DLS), and their efficacy in gene  
3 expression was determined by luminance spectrometry and flow cytometry.  
4  
5  
6

## 7 8 9 **2. Materials and Methods**

### 10 *2.1. Plasmid DNA*

11  
12 The plasmid DNAs used in the study were pEGFP-N2 (4.7 kb, coding an enhanced  
13 green fluorescence protein reporter gene, Clontech, Palo Alto, CA, USA) and pGL4.13 (4.6  
14 kb, coding a firefly luciferase reporter gene, Promega, Madison, WI, USA). pEGFP-N2 and  
15 pGL4.13 were amplified using DH5 $\alpha$  and purified by Qiagen Plasmid Mega Kit (Valencia,  
16 CA, USA) according to the manufacturer's instructions. The purity of plasmids was  
17 analyzed by gel electrophoresis (0.8% agarose), while their concentration was measured by  
18 UV absorption at 260 nm (Jasco, Tokyo, Japan).  
19  
20  
21  
22  
23  
24  
25  
26  
27

### 28 *2.2. Preparation of test complexes*

29  
30 The charge ratio (N/P/C) of test complexes was expressed as the ratio of moles of the  
31 amino groups (N) on CS to the phosphate groups (P) on DNA and the carboxyl groups (C)  
32 on  $\gamma$ -PGA. Test complexes at N/P/C molar ratios of 10/1/0 (CS/DNA complexes) and  
33 10/1/4 (CS/DNA/ $\gamma$ -PGA complexes) were prepared by an ionic-gelation method  
34 [7]. Briefly, an aqueous DNA (pEGFP-N2 or pGL4.13, 33  $\mu$ g) was mixed with an aqueous  
35  $\gamma$ -PGA (20 kDa, 0 or 51.2  $\mu$ g, Vedan, Taichung, Taiwan) with a final volume of 100  
36  $\mu$ l. Test complexes were obtained upon addition of the mixed solution, using a pipette, into  
37 an aqueous CS (15 kDa, with a degree of deacetylation of 85%, 0.2  $\mu$ g/ $\mu$ l, 100  $\mu$ l, pH 6.0,  
38 Challenge Bioproducts, Taichung, Taiwan) and then thoroughly mixed for 30–60 s by vortex  
39 and left for at least 1 h at room temperature. The morphology of the obtained complexes  
40 was examined by TEM (JEOL, Tokyo, Japan) [8].  
41  
42  
43  
44  
45  
46  
47  
48  
49  
50  
51  
52  
53

### 54 *2.3. In vitro transfection*

55  
56 HT1080 (human fibrosarcoma) cells were cultured in DMEM media supplemented with  
57 2.2 g/l sodium bicarbonate and 10% fetal bovine serum (FBS). Cells were subcultured  
58  
59  
60  
61  
62  
63  
64  
65

1 according to ATCC recommendations without using any antibiotics. For transfection, cells  
2 were seeded on 12-well plates at  $2 \times 10^5$  cells/well and transfected the next day at 50–80%  
3 confluency. Prior to transfection, the media were removed and cells were rinsed twice with  
4 transfection media (DMEM without FBS, pH 6.0). Cells were replenished with 0.6 ml  
5 transfection media containing test complexes at a concentration of 2  $\mu$ g DNA/well.  
6  
7  
8  
9

10  
11 At 2 h post transfection, the transfection media containing test complexes were  
12 removed, the cells rinsed twice with transfection media and refilled with FBS-containing  
13 media until analysis at 48 h after transfection. Cells were then observed under a  
14 fluorescence microscope (Carl Zeiss Optical, Chester, VA, USA) to monitor any  
15 morphological changes and to obtain an estimate of the transfection efficiency. Cells  
16 transfected with Lipofectamine<sup>TM</sup> 2000 (Invitrogen, Carlsbad, CA, USA) were used as a  
17 positive control and those without any treatment were used as a negative  
18 control. Transfection efficiencies were presented by two numeric indicators: percentage of  
19 cells transfected and gene expression level [9].  
20  
21  
22  
23  
24  
25  
26  
27  
28  
29

#### 30 *2.4. Percentage of cells transfected*

31  
32 The percentage of cells transfected was quantitatively assessed at 48 h after transfection  
33 by flow cytometry. Cells were detached by 0.025% trypsin-EDTA. Cell suspensions were  
34 then transferred to microtubes, fixed by 4% paraformaldehyde and determined the  
35 transfection efficiency by a flow cytometer (Beckman Coulter, Fullerton, CA, USA)  
36 equipped with a 488-nm argon laser for excitation. For each sample, 10,000 events were  
37 collected and fluorescence was detected. Signals were amplified in logarithmic mode for  
38 fluorescence to determine the EGFP positive events by a standard gating technique. The  
39 percentage of positive events was calculated as the events within the gate divided by the total  
40 number of events, excluding cell debris.  
41  
42  
43  
44  
45  
46  
47  
48  
49  
50

#### 51 *2.5. Gene expression level*

52  
53 The gene expression levels of cells were assayed by quantifying the expressions of  
54 EGFP or luciferase. The expression level of EGFP was quantified by comparing mean  
55 fluorescence of  $2 \times 10^5$  cells. Briefly, cells were treated with test complexes containing  
56  
57  
58  
59  
60  
61  
62  
63  
64  
65

1 pEGFP-N2. After 48 h, cells were detached and analyzed by flow cytometry as described in  
2  
3 Section 2.4.  
4

5 For the expression of luciferase, cells were plated on 24-well plates (with a seeding  
6 density of  $1 \times 10^5$  cells) and transfected as described in Section 2.3 with the exception that 1  
7  $\mu\text{g}$  pGL4.13 was used. The cells transfected were lysed by 100  $\mu\text{l}$  of passive lysis buffer  
8 (Promega). The cell lysate was transferred into a 1.5-ml microtube, while the cell debris  
9 was separated by centrifugation (14,000 rpm, 5 min). Subsequently, a 100  $\mu\text{l}$  of the  
10 luciferase assay reagent (Promega) was added to a 20  $\mu\text{l}$  of the supernatant and the relative  
11 luminescence of the sample was determined by a microplate luminometer (Berthold  
12 Technologies, Bad Wildbad, Germany) and normalized to the total cell protein concentration  
13 by the Bradford method.  
14  
15  
16  
17  
18  
19  
20  
21  
22  
23

#### 24 *2.6. Fluorescent complex preparation and flow-cytometry analysis*

25  
26 Cy3-labeled CS (Cy3-CS) and FITC-labeled CS (FITC-CS) were synthesized as per the  
27 methods described in the literature [10,11]. To remove the unconjugated Cy3 and FITC, the  
28 synthesized Cy3-CS and FITC-CS were dialyzed in the dark against deionized (DI) water  
29 and replaced on a daily basis until no fluorescence was detected in the supernatant. The  
30 resultant Cy3-CS and FITC-CS were lyophilized in a freeze dryer. Cy3- and FITC-labeled  
31 complexes were then prepared as described in Section 2.2.  
32  
33  
34  
35  
36  
37  
38

39 To quantify the cellular uptake of test complexes, cells were plated on 12-well plates  
40 and transfected with FITC-labeled complexes at a concentration of 2  $\mu\text{g}$  DNA/well for 2  
41 h. After transfection, cells were detached by 0.025% trypsin-EDTA and transferred to  
42 microtubes. Subsequently, cells were resuspended in phosphate buffered saline (PBS)  
43 containing 1mM EDTA and fixed in 4% paraformaldehyde. Finally, the cells were analyzed  
44 by flow cytometry as described in Section 2.4.  
45  
46  
47  
48  
49  
50

#### 51 *2.7. MD simulations*

52  
53 MD simulations of the self-assembly of CS and  $\gamma$ -PGA in complexation were  
54 performed by a MD method [12]. MD simulations were accomplished with the program  
55 NAMD [13] using parameters adapted from the CHARMM 27 force field [14]. The  
56  
57  
58  
59  
60  
61  
62  
63  
64  
65

1 models were minimized to remove unfavorable contacts, brought to 310 K by velocity  
2 rescaling and equilibrated for 1 ns. Before any MD trajectory was run, 40 ps of energy  
3 minimization were performed to relax the conformational and structural tensions. This  
4 minimum structure was the starting point for the MD simulations. For this purpose, the  
5 molecule was embedded into a cubic simulation box of 80 Å. A cutoff distance of 12 Å  
6 was employed for the nonbonded and electrostatic interactions. The heating process was  
7 performed from 0 to 310 K through Langevin damping with a coefficient of 10 ps<sup>-1</sup>. A time  
8 step of 2 fs was employed for rescaling the temperature. After 20 ps heating to 310 K,  
9 equilibration trajectories of 1 ns were recorded, which provided the data for the structural  
10 and thermodynamic evaluations. The equations of motion were integrated with the Shake  
11 algorithm with a time step of 1 fs. Figures displaying atomistic pictures of molecules with  
12 hydrogen bondings were generated using UCSF Chimera [15].

## 26 *2.8. Endocytosis inhibition*

28 To study the effect of various inhibitors on the uptake of test complexes, cells were  
29 pre-incubated with the following inhibitors individually at concentrations which were not  
30 toxic to the cells: 10 µg/ml of chlorpromazine [16], 50nM wortamannin [17], 5 µg/ml  
31 cytochalasin D [18], 5 µg/ml filipin [19] or 200µM genistein [19,20]; the MTT assay [16]  
32 was employed to confirm their toxicity. In the study, the group without any treatment was  
33 used as a background in the flow cytometry analysis, while the groups in the presence of test  
34 complexes but without inhibitor treatment were used as controls and their fluorescence  
35 intensities were expressed as 100%. Following pre-incubation for 30 min, the inhibitor  
36 solutions were removed, and the freshly prepared test complexes (FITC-labeled) in media  
37 containing inhibitors at the same concentrations were added and further incubated for 2  
38 h. Subsequently, cells were washed three times with PBS, collected according to the  
39 methods described above and analyzed by flow cytometry.

## 54 *2.9. Examination of internalization of test complexes by TEM*

56 To directly observe the mechanism of cellular internalization, cells were incubated with  
57 test complexes at 37°C. After washing three times with PBS, cells were fixed for 30 min at  
58

1 room temperature in 2% paraformaldehyde and 2.5% glutaraldehyde in 0.1M cacodylate  
2 buffer at pH 7.4. The cells were rinsed twice in the same buffer with 6.8% sucrose and  
3 subsequently postfixed in 1% OsO<sub>4</sub>. After rinsing followed by dehydration in graded  
4 alcohol series, the cells were embedded in Spurr resin and polymerized at 70°C  
5 overnight. Ultrathin sections were then cut with a diamond knife and loaded onto TEM  
6 grids. The sections were examined by a Philips CM10 electron microscope at accelerating  
7 voltage of 120 kV and micrographs were taken [21].  
8  
9

### 10 2.10. Intracellular trafficking

11 To study the intracellular trafficking, cells were treated with the Cy3-labeled test  
12 complexes in the serum-free medium. After incubation for 1.5 h, cells were washed twice  
13 with the pre-warmed PBS and then treated with 50nM LysoTracker (HCK-123, InvitroGene,  
14 Carlsbad, CA, USA) for 30 min at 37°C following the supplier's protocol and examined  
15 using CLSM (TCS SL, Leica, Germany).  
16

### 17 2.11. Statistical analysis

18 Comparison between groups was analyzed by the one-tailed Student's *t*-test (SPSS,  
19 Chicago, Ill, USA). All data are presented as a mean value with its standard deviation  
20 indicated (mean ± SD). Differences were considered to be statistically significant when the  
21 *P* values were less than 0.05.  
22  
23  
24  
25  
26  
27  
28  
29

## 30 3. Results and Discussion

31 CS/DNA complexes (a binary system) generally transfect cells more efficiently than  
32 naked DNA but less than commercially available liposome formulations [22]. It has been  
33 suggested that the strength of electrostatic interactions between CS and DNA prevent their  
34 dissociation within cells, thus precluding transcription of DNA and resulting in low  
35 transfection [1,2]. In a previous study, we demonstrated that after the incorporation of  
36  $\gamma$ -PGA in CS/DNA complexes (a ternary system), the percentage of cells transfected and  
37 their gene level expressed were significantly enhanced [5]. Additionally, Kurosaki *et al.*  
38 reported that cationic complexes coated with the negatively charged  $\gamma$ -PGA not only reduced  
39  
40  
41  
42  
43  
44  
45  
46  
47  
48  
49  
50  
51  
52  
53  
54  
55  
56  
57  
58  
59  
60  
61  
62  
63  
64  
65

1 their cytotoxicity but also significantly improved their efficiency in gene expression [6].  
2  
3 Generally, anionic complexes are not taken up well by cells because of the electrostatic  
4  
5 repulsion induced by the negatively charged cell membranes. Therefore, the ternary  
6  
7 complexes containing  $\gamma$ -PGA must have different mechanisms in cellular uptake and  
8  
9 intracellular fate from their binary counterparts.

### 10 11 *3.1. Characterization of test complexes*

12  
13 In the study, test complexes were prepared with an N/P/C ratio of 10/1/0 (binary  
14  
15 CS/DNA complexes) or 10/1/4 (ternary CS/DNA/ $\gamma$ -PGA complexes). The binding capacity  
16  
17 of CS with DNA prepared at various N/P ratios was evaluated in our previous study using  
18  
19 the gel retardation assay [5]. The results showed that as the N/P ratio was increased to 10/1,  
20  
21 the migration of DNA was retarded completely. By incorporating  $\gamma$ -PGA in CS/DNA  
22  
23 complexes, no significant DNA release was observed. However, as the amount of  $\gamma$ -PGA  
24  
25 incorporated was increased to a critical value (N/P/C ratio of 10/1/6), the transfection  
26  
27 efficiency of CS/DNA/ $\gamma$ -PGA complexes started to drop appreciably [5].  
28  
29

30  
31 TEM was used to examine the morphology of test complexes. As shown in Fig 1, the  
32  
33 binary CS/DNA complexes had an irregular shape, while the ternary CS/DNA/ $\gamma$ -PGA  
34  
35 complexes were spherical in shape. Our previous SAXS results indicated that test  
36  
37 complexes formed by the ternary system were composed of two types of domains containing  
38  
39 CS/DNA and CS/ $\gamma$ -PGA complexes [5], as schematically illustrated in Fig 1. The particle  
40  
41 size and zeta potential of CS/DNA (CS/DNA/ $\gamma$ -PGA) complexes measured by DLS were  
42  
43  $140.2 \pm 7.7$  nm ( $152.5 \pm 5.1$  nm) and  $31.7 \pm 0.8$  mV ( $28.7 \pm 1.2$  mV), respectively (n = 5  
44  
45 batches). The encapsulation efficiencies of DNA in test complexes for both studied groups  
46  
47 were about the same and approached 100%.  
48

### 49 50 *3.2. Cellular uptake and transfection efficiency*

51  
52 After pre-incubation of the cells with test complexes for different time periods (i.e.,  
53  
54 distinct durations of internalization or transfection), their successful expression of delivered  
55  
56 DNA at 48 h post transfection was reflected by luciferase gene expression levels. As  
57  
58 shown in Fig. 2a, cells transfected with CS/DNA or CS/DNA/ $\gamma$ -PGA complexes produced a  
59  
60  
61  
62  
63  
64  
65

1 gradient increase of luciferase expression as the internalization time progressed. The  
2 luciferase gene expression levels for cells incubated with CS/DNA/ $\gamma$ -PGA complexes were  
3 consistently higher than their CS/DNA counterparts throughout the entire time course of the  
4 study ( $P < 0.05$ ).  
5  
6  
7

8  
9 To visualize the cellular uptake, CS was fluorescently labeled with FITC. The  
10 percentage of cells that internalized the FITC-labeled test complexes (Fig 2b) and their  
11 fluorescence intensity (Fig. 2c) were quantified by flow cytometry at 2 h after transfection.  
12 Compared to those transfected with CS/DNA complexes, the percentage of fluorescent cells  
13 and their fluorescence intensity in the group treated with CS/DNA/ $\gamma$ -PGA complexes were  
14 significantly enhanced ( $P < 0.05$ ), an indication of a greater cellular uptake.  
15  
16  
17  
18  
19  
20  
21

22 To determine the percentage of cells that actually expressed the transgene, we counted  
23 the number of EGFP-positive cells using flow cytometry at 48 h post transfection. As  
24 shown in Fig. 2d, 15% of the cells produced EGFP when transfected with CS/DNA  
25 complexes. By incorporating  $\gamma$ -PGA in complexes (CS/DNA/ $\gamma$ -PGA), an approximately  
26 4-fold increase in the percentage of EGFP-positive cells was found (55%,  $P < 0.05$ ).  
27  
28  
29  
30  
31

### 32 3.3. MD simulations

33  
34 MD simulations were performed in a full-atom model to gain insight into the role that  
35  $\gamma$ -PGA may play in assisting the cellular uptake. Both CS and  $\gamma$ -PGA molecules  
36 considered in the MD simulations contained 10 monomer units. The present atomistic  
37 simulation would allow the capture of the self-assembly of CS and  $\gamma$ -PGA in complexation.  
38 The methodology adopted has recently been applied to enable simulations of the  
39 self-assembly of protein and detergent into mixed micelles [23,24]. As shown in Fig. 3a,  
40 free  $\gamma$ -PGA forms an intramolecular hydrogen bonding between the amine group ( $-\text{NH}_2$ ) of  
41 the N-terminal glutamyl unit and the carbonyl group ( $-\text{C}=\text{O}$ ) on its neighboring unit; thus,  
42 the terminal amine group on  $\gamma$ -PGA is hidden. In contrast, after forming complexes, the  
43 amine groups on CS may form intermolecular hydrogen bondings with the carbonyl groups  
44 of  $\gamma$ -PGA; therefore, the hidden amine group in the N-terminal  $\gamma$ -glutamyl unit on  $\gamma$ -PGA is  
45 exposed (Fig. 3b).  
46  
47  
48  
49  
50  
51  
52  
53  
54  
55  
56  
57  
58  
59  
60  
61  
62  
63  
64  
65

1 The exposure of the free N-terminal  $\gamma$ -glutamyl unit of  $\gamma$ -PGA on the surface of  
2 CS/ $\gamma$ -PGA complexes (Fig. 3b) may enhance its interaction with the enzyme  $\gamma$ -glutamyl  
3 transpeptidase (GGT), which is localized in the cell membrane and exerts the only specificity  
4 to those substrates containing free  $\gamma$ -glutamic acids in their N-terminal ends [25]. It has  
5 been reported that GGT can use a wide variety of  $\gamma$ -glutamyl compounds as substrates [26].  
6 The most popular case of GGT substrates is glutathione; GGT may cleave the  $\gamma$ -glutamyl  
7 bond of extracellular glutathione, enabling the cell to use extracellular glutathione as a  
8 source of cysteine to increase the synthesis of intracellular glutathione [27]. In CS/ $\gamma$ -PGA  
9 complexes,  $\gamma$ -PGA displays a free  $\gamma$ -glutamic acid in its N-terminal end and thus may be  
10 recognized by GGT in the cell membrane, resulting in a significant increase in their cellular  
11 uptake (Fig. 2b and 2c). The detailed mechanism may need further investigation.  
12  
13  
14  
15  
16  
17  
18  
19  
20  
21  
22  
23

24 The results discussed in Sections 3.2 and 3.3 suggest that with the incorporation of  
25  $\gamma$ -PGA, the cellular uptake and transgene expression of CS/DNA complexes were  
26 significantly enhanced. In a previous study, we demonstrated that there are different  
27 pathways involved in the internalization of CS/DNA and CS/DNA/ $\gamma$ -PGA complexes; the  
28 former is trypsin concentration-independent and the latter trypsin concentration-dependent  
29 [5]. However, their exact mechanisms in endocytosis and intracellular trafficking remain to  
30 be understood. Understanding the fate of complexes with respect to their uptake pattern  
31 and the intracellular localization is crucial in designing a new genetic or drug carrier [28].  
32  
33  
34  
35  
36  
37  
38  
39  
40

#### 41 *3.4. Endocytosis pathways of CS/DNA and CS/DNA/ $\gamma$ -PGA complexes*

42

43 A variety of forms of endocytosis have been demonstrated to be involved in the cellular  
44 uptake of polyplexes [16,20]. Current evidences suggest that endocytosis is the main mode  
45 of CS-based complexes entering into the cells [29]. To elucidate their potential cellular  
46 uptake pathways, the interactions between CS/DNA or CS/DNA/ $\gamma$ -PGA complexes and cell  
47 membranes were investigated by treating cells with different chemical inhibitors of  
48 clathrin-mediated endocytosis, caveolae-mediated endocytosis and macropinocytosis and  
49 then analyzed by flow cytometry. It has been reported that a narrow concentration range of  
50 specific inhibitory function and nonspecific toxicity exists [16]. We therefore first  
51  
52  
53  
54  
55  
56  
57  
58  
59  
60  
61  
62  
63  
64  
65

1 determined the cytotoxicity of the concentration of each inhibitor used in the subsequent  
2 transfection experiments. As shown in Fig. 4, the concentration of each inhibitor used in  
3 the study did not significantly reduce the cell viability (> 94% of control). These data  
4 ensure that the reductions in cellular uptake to be discussed in Fig. 5a and 5b are specific to  
5 the inhibitors, rather than the cytotoxicity of inhibitors.  
6  
7  
8  
9

10  
11 Fig. 5a and 5b presents the results of the internalization of CS/DNA and  
12 CS/DNA/ $\gamma$ -PGA complexes by cells in the presence of various inhibitors; their counterparts  
13 in the absence of inhibitors were used as controls. The inhibition of clathrin-mediated  
14 uptake was tested by using the cationic amphiphilic drug chlorpromazine, which causes  
15 clathrin to accumulate in late endosomes, thereby inhibiting coated pit endocytosis [20,30].  
16 Compared with the controls, the cellular uptake of both test complexes increased relatively  
17 in the presence of chlorpromazine (Fig. 5b). Increase in cellular uptake after inhibitor  
18 treatment has also been reported by other investigators [20]. It is possible that other  
19 cellular uptake pathways that are not normally involved may be up-regulated in the presence  
20 of inhibitors. These results indicate that the clathrin-mediated pathway was not involved in  
21 the internalization of CS/DNA and CS/DNA/ $\gamma$ -PGA complexes.  
22  
23  
24  
25  
26  
27  
28  
29  
30  
31  
32  
33

34 Wortmannin is a phosphatidyl inositol-3-phosphate inhibitor [17], while cytochalasin D  
35 can inhibit actin polymerization and membrane ruffling [20]; both are known to be involved  
36 in macropinocytosis. Relative to the control, the reduction in internalization of CS/DNA  
37 complexes by cells pre-treated with wortmannin (cytochalasin D) was 3% (8%), implying  
38 that a minor fraction of test complexes could be internalized via micropinocytosis. In  
39 contrast, a greater degree of inhibition in cellular uptake of CS/DNA/ $\gamma$ -PGA complexes was  
40 observed (20% and 30% for the cells pre-treated with wortmannin and cytochalasin D,  
41 respectively,  $P < 0.05$ ), suggesting that the incorporation of  $\gamma$ -PGA in CS/DNA complexes  
42 significantly enhanced their internalization by macropinocytosis.  
43  
44  
45  
46  
47  
48  
49  
50  
51  
52  
53

54 Caveolae, a specialized type of lipid rafts, are flask-shaped invaginations in the plasma  
55 membrane enriched in proteins as well as cholesterol and spingolipids [31,32]. To discern  
56 any role that caveolae-mediated endocytosis may play in cellular uptake, two inhibitors,  
57  
58  
59  
60  
61  
62  
63  
64  
65

1 filipin and genistein, were used. Filipin (a sterol-binding pentaene macrolide antibiotic)  
2 selectively inhibits caveolae invagination by the formation of cholesterol precipitates, while  
3 genistein (a tyrosine kinase inhibitor) is used to block lipid raft-mediated endocytosis [16].  
4  
5 It has been reported that cholesterol and lipid rafts are involved in membrane trafficking  
6  
7 [19,33].  
8  
9

10  
11 As shown in Fig. 5a and 5b, treating cells with fillipin prior to incubation with CS/DNA  
12 or CS/DNA/ $\gamma$ -PGA complexes increased their cellular uptake. In contrast, cells pretreated  
13 with genistein resulted in a significant inhibition of the number of cells internalized [55%  
14 reduction for CS/DNA complexes and an enhanced reduction of 90% with the incorporation  
15 of  $\gamma$ -PGA (CS/DNA/ $\gamma$ -PGA)]. These data suggest that the internalization of both test  
16 complexes was caveolae-dependent and related with the lipid raft-mediated route, but not  
17 through the inhibition of invagination of caveolae.  
18  
19

20  
21 The aforementioned results clearly show that the internalization of CS/DNA complexes  
22 took place by a combination of mechanisms, macropinocytosis and caveolae-mediated  
23 pathways at least; by incorporating  $\gamma$ -PGA in complexes (CS/DNA/ $\gamma$ -PGA), both uptake  
24 pathways were further enhanced. To further determine the effect of the internalization  
25 pathway on their transgene expression, the transfection efficiencies of CS/DNA/ $\gamma$ -PGA  
26 complexes (EGFP gene) in the presence of distinct inhibitors were studied. As shown in  
27 Fig. 5c, in the presence of wortmannin and cytochalasin D (macropinocytosis inhibitors), the  
28 transfection efficiencies of CS/DNA/ $\gamma$ -PGA complexes were reduced by 55% and 75%,  
29 respectively, while their transfection efficiency was suppressed by 90% when using a  
30 caveolae-mediated-pathway inhibitor, genistein ( $P < 0.05$ ). These data suggest that  
31 caveolae-mediated pathway played a major role in the cellular uptake of CS/DNA/ $\gamma$ -PGA  
32 complexes and their subsequent transgene expression.  
33  
34

35  
36 TEM was used to gain directly understanding of the mechanisms of internalization of  
37 CS/DNA and CS/DNA/ $\gamma$ -PGA complexes. As shown in Fig. 6a, macropinocytosis exerted  
38 its influence on the internalization of CS/DNA complexes. During macropinocytosis,  
39 membrane ruffling occurs; that is, the rims of the membrane folds extending from the  
40  
41  
42  
43  
44  
45  
46  
47  
48  
49  
50

1 surface fuse back with the plasma membrane [34]. Additionally, TEM micrographs  
2 revealed flask-shaped caveolae in the plasma membrane (Fig. 6b and 6c), an indication of  
3 caveolae-dependent endocytosis [31]. Similar pathways were observed in the  
4 internalization of CS/DNA/ $\gamma$ -PGA complexes: the formation of lamellipodia (Fig. 6d and 6e)  
5 and caveolae-derived endocytic vesicles (Fig. 6f). These findings were consistent with  
6 those observed in the inhibition experiments (Fig. 5a and 5b).  
7  
8  
9  
10  
11  
12

### 13 *3.5. Intracellular trafficking of test complexes*

14  
15 To track test complexes following their uptake, cells were treated with Cy3-labeled  
16 CS/DNA and CS/DNA/ $\gamma$ -PGA complexes individually and subsequently stained with  
17 LysoTracker; the intracellular localization of test complexes was followed by CLSM. At 2 h  
18 after transfection, accumulation of Cy3-labeled complexes (red dots) was observed in most  
19 of the incubated cells in both studied groups (Fig. 7a); some complex aggregates were found  
20 entrapped within the lysosomal vesicles (green dots). The co-localization of test complexes  
21 with lysosomes produced a yellow fluorescence in the merged images. Interestingly,  
22 although there were more red dots (a greater cellular uptake) seen in the cytoplasm in the  
23 group treated with CS/DNA/ $\gamma$ -PGA complexes when compared with that transfected with  
24 CS/DNA complexes, a less percentage of their co-localization with lysosomes (yellow dots)  
25 was observed (50% for CS/DNA complexes vs. 30% for CS/DNA/ $\gamma$ -PGA complexes, Fig.  
26 7b).  
27  
28  
29  
30  
31  
32  
33  
34  
35  
36  
37  
38  
39  
40

41 Degradation of complexes in lysosomes is one of the barriers for non-viral vectors  
42 mediated gene delivery [35]. It has been reported that macropinosomes can acidify but do  
43 not intersect with lysosomes, thus representing a potential alternative cell entry route of gene  
44 transfer for the avoidance of lysosomal degradation [36]. Additionally, the  
45 caveolae-mediated pathway has been proposed to be advantageous over the  
46 clathrin-mediated pathway for transfection DNA due to its possible avoidance of lysosomal  
47 degradation [35]. Some pathogens that use caveolae as their portal of entry escape delivery  
48 to and digestion in lysosomes [37]; it is thought that caveosomes lack the proper signal  
49 molecules required for interaction with other cellular compartments [38]. Compared with  
50  
51  
52  
53  
54  
55  
56  
57  
58  
59  
60  
61  
62  
63  
64  
65

1 their CS/DNA counterparts, a greater cellular uptake together with a less entry into  
2 lysosomes might explain the promotion of transfection efficiency of CS/DNA/ $\gamma$ -PGA  
3 complexes (Fig. 8).  
4  
5  
6  
7  
8

#### 9 **4. Conclusions**

10 The cellular uptake of CS-based complexes was significantly enhanced via the  
11 incorporation of  $\gamma$ -PGA. CS/DNA complexes were internalized via macropinocytosis and  
12 caveolae-mediated pathway. By incorporating  $\gamma$ -PGA in complexes (CS/DNA/ $\gamma$ -PGA),  
13 both pathways were significantly enhanced; however, the caveolae-mediated pathway played  
14 a major role. After internalization, the percentage of CS/DNA/ $\gamma$ -PGA complexes entry into  
15 lysosomes was significantly less than their CS/DNA counterpart and thus had an enhanced  
16 gene expression level. Knowledge of these mechanisms is critical for the development of  
17 efficient vectors for DNA transfection.  
18  
19  
20  
21  
22  
23  
24  
25  
26  
27  
28  
29

#### 30 **Acknowledgment**

31 This work was supported by a grant from the National Science Council (NSC  
32 99-2120-M-007-006), Taiwan, Republic of China.  
33  
34  
35  
36  
37  
38  
39  
40  
41  
42  
43  
44  
45  
46  
47  
48  
49  
50  
51  
52  
53  
54  
55  
56  
57  
58  
59  
60  
61  
62  
63  
64  
65

1 **References**

- 2
- 3 [1] Mao HQ, Roy K, Troung-Le VL, Janes KA, Lin KY, Wang Y, et al. Chitosan-DNA
- 4 nanoparticles as gene carriers: Synthesis, characterization and transfection efficiency. *J*
- 5 *Control Release* 2001;70:399–421.
- 6
- 7
- 8
- 9 [2] Kim TH, Park IK, Nah JW, Choi YJ, Cho CS. Galactosylated chitosan/DNA
- 10 nanoparticles prepared using water-soluble chitosan as a gene carrier. *Biomaterials*
- 11 2004;25:3783–92.
- 12
- 13
- 14
- 15 [3] Morille M, Passirani C, Vonarbourg A, Clavreul A, Benoit JP. Progress in developing
- 16 cationic vectors for non-viral systemic gene therapy against cancer. *Biomaterials*
- 17 2008;29:3477–96.
- 18
- 19
- 20
- 21 [4] Kim TH, Jiang HL, Jere D, Park IK, Cho MH, Nah JW, et al. Chemical modification of
- 22 chitosan as a gene carrier in vitro and in vivo. *Prog Polym Sci* 2007;32:726–53.
- 23
- 24
- 25 [5] Peng SF, Yang MJ, Su CJ, Chen HL, Lee PW, Wei MC, et al. Effects of incorporation of
- 26 poly( $\gamma$ -glutamic acid) in chitosan/DNA complex nanoparticles on cellular uptake and
- 27 transfection efficiency. *Biomaterials* 2009;30:1797–808.
- 28
- 29
- 30
- 31 [6] Kurosaki T, Kitahara T, Fumoto S, Nishida K, Nakamura J, Niidome T, et al. Ternary
- 32 complexes of pDNA, polyethylenimine, and  $\gamma$ -polyglutamic acid for gene delivery
- 33 systems. *Biomaterials* 2009;30:2846–53.
- 34
- 35
- 36 [7] Lee PW, Peng SF, Su CJ, Mi FL, Chen HL, Wei MC, et al. The use of biodegradable
- 37 polymeric nanoparticles in combination with a low-pressure gene gun for transdermal
- 38 DNA delivery. *Biomaterials* 2008;29:742–51.
- 39
- 40
- 41 [8] Adams CWM. Osmium tetroxide and the marchi method: Reactions with polar and
- 42 non-polar lipids, protein and polysaccharide. *J Histochem Cytochem* 1960;8:262–7.
- 43
- 44
- 45 [9] Ko IK, Ziady A, Lu S, Kwon YJ. Acid-degradable cationic methacrylamide polymerized
- 46 in the presence of plasmid DNA as tunable non-viral gene carrier. *Biomaterials*
- 47 2008;29:3872–81.
- 48
- 49
- 50 [10] Qaqish RB, Amiji MM. Synthesis of a fluorescent chitosan derivative and its
- 51 application for the study of chitosan-mucin interactions. *Carbohydr Polym*
- 52
- 53
- 54
- 55
- 56
- 57
- 58
- 59
- 60
- 61
- 62
- 63
- 64
- 65

1999;38:99–107.

- 2  
3 [11] Ho YP, Chen HH, Leong KW, Wang TH. Evaluating the intracellular stability and  
4 unpacking of DNA nanocomplexes by quantum dots-FRET. *J Control Release*  
5 2006;116:83–9.  
6  
7  
8  
9 [12] Marrink SJ, de Vries AH, Mark AE. Coarse grained model for semiquantitative lipid  
10 simulations. *J Phys Chem B* 2004;108:750–60.  
11  
12 [13] Nelson MT, Humphrey W, Gursoy A, Dalke A, Kale LV, Skeel RD, et al. NAMD: A  
13 parallel, object oriented molecular dynamics program. *Int J Supercomput Appl High*  
14 *Perform Comput* 1996;10:251–68.  
15  
16 [14] Brooks BR, Bruccoleri RE, Olafson BD, States DJ, Swaminathan S, Karplus M.  
17 Charmm: A program for macromolecular energy, minimization, and dynamics  
18 calculations. *J Comput Chem* 1983;4:187–217.  
19  
20 [15] Pettersen EF, Goddard TD, Huang CC, Couch GS, Greenblatt DM, Meng EC, et al.  
21 UCSF Chimera-- A visualization system for exploratory research and analysis. *J*  
22 *Comput Chem* 2004;25:1605–12.  
23  
24 [16] Von Gersdorff K, Sanders NN, Vandenbroucke R, De Smedt SC, Wagner E, Ogris M.  
25 The internalization route resulting in successful gene expression depends on both cell  
26 line and polyethylenimine polyplex type. *Mol Ther* 2006;14:745–53.  
27  
28 [17] Araki N, Johnson MT, Swanson JA. A role for phosphoinositide 3-kinase in the  
29 completion of macropinocytosis and phagocytosis by macrophages. *J Cell Biol*  
30 1996;135:1249–60.  
31  
32 [18] Parton RG, Joggerst B, Simons K. Regulated internalization of caveolae. *J Cell Biol*  
33 1994;127:1199–215.  
34  
35 [19] Manunta M, Tan PH, Sagoo P, Kashefi K, George AJT. Gene delivery by dendrimers  
36 operates via a cholesterol dependent pathway. *Nucleic Acids Res* 2004;32:2730–9.  
37  
38 [20] Perumal OP, Inapagolla R, Kannan S, Kannan RM. The effect of surface functionality  
39 on cellular trafficking of dendrimers. *Biomaterials* 2008;29:3469–76.  
40  
41 [21] Koziara JM, Whisman TR, Tseng MT, Mumper RJ. In-vivo efficacy of novel paclitaxel  
42  
43  
44  
45  
46  
47  
48  
49  
50  
51  
52  
53  
54  
55  
56  
57  
58  
59  
60  
61  
62  
63  
64  
65

- 1 nanoparticles in paclitaxel-resistant human colorectal tumors. *J Control Release*  
2  
3 2006;112:312–9.  
4
- 5 [22] Douglas KL, Piccirillo CA, Tabrizian M. Effects of alginate inclusion on the vector  
6  
7 properties of chitosan-based nanoparticles. *J Control Release* 2006;115:354–61.  
8
- 9 [23] Bond PJ, Holyoake J, Ivetac A, Khalid S, Sansom MSP. Coarse-grained molecular  
10  
11 dynamics simulations of membrane proteins and peptides. *J Struct Biol*  
12  
13 2007;157:593–605.  
14
- 15 [24] Bond PJ, Sansom MSP. Insertion and assembly of membrane proteins via simulation. *J*  
16  
17 *Am Chem Soc* 2006;128:2697–704.  
18
- 19 [25] Lieberman MW, Barrios R, Carter BZ, Habib GM, Lebovitz RM, Rajagopa-Ian S, et al.  
20  
21 Gamma-glutamyl transpeptidase: What does the organization and expression of a  
22  
23 multipromoter gene tell us about its functions? *Am J Pathol* 1995;147:1175–85.  
24
- 25 [26] Magnan SDJ, Shirota FN, Nagasawa HT. Drug latentiation by  $\gamma$ -glutamyl transpeptidase.  
26  
27 *J Med Chem* 1982;25:1018–21.  
28
- 29 [27] Hanigan MH. Gamma-glutamyl transpeptidase, a glutathionase: Its expression and  
30  
31 function in carcinogenesis. *Chem Biol Interact* 1998;111–112:333–42.  
32  
33
- 34 [28] Rejman J, Conese M, Hoekstra D. Gene transfer by means of lipo- and polyplexes:  
35  
36 Role of clathrin and caveolae-mediated endocytosis. *J Liposome Res* 2006;16:237–47.  
37  
38
- 39 [29] Douglas KL, Piccirillo CA, Tabrizian M. Cell line-dependent internalization pathways  
40  
41 and intracellular trafficking determine transfection efficiency of nanoparticle vectors.  
42  
43 *Eur J Pharm Biopharm* 2008;68:676–87.  
44
- 45 [30] Khalil IA, Kogure K, Akita H, Harashima H. Uptake pathways and subsequent  
46  
47 intracellular trafficking in nonviral gene delivery. *Pharmacol Rev* 2006;58:32–45.  
48
- 49 [31] Parton RG, Simons K. The multiple faces of caveolae. *Nat Rev Mol Cell Biol*  
50  
51 2007;8:185–94.  
52
- 53 [32] Mayor S, Pagano RE. Pathways of clathrin-independent endocytosis. *Nat Rev Mol Cell*  
54  
55 *Biol* 2007;8:603–12.  
56
- 57 [33] Jacobson K, Mouritsen OG, Anderson RGW. Lipid rafts: At a crossroad between cell  
58  
59  
60  
61  
62  
63  
64  
65

1 biology and physics. *Nat Cell Biol* 2007;9:7–14.

2  
3 [34] Mellman I. Endocytosis and molecular sorting. *Annu Rev Cell Dev Biol*  
4  
5 1996;12:575–625.

6  
7 [35] Rejman J, Bragonzi A, Conese M. Role of clathrin- and caveolae-mediated endocytosis  
8  
9 in gene transfer mediated by lipo- and polyplexes. *Mol Ther* 2005;12:468–74.

10  
11 [36] Conner SD, Schmid SL. Regulated portals of entry into the cell. *Nature*  
12  
13 2003;422:37–44.

14  
15 [37] Shin JS, Abraham S N. Caveolae as portals of entry for microbes. *Microbes Infect*  
16  
17 2001;3:755–61.

18  
19 [38] Joiner KA, Fuhrman SA, Miettinen HM, Kasper LH, Mellman I. *Toxoplasma gondii*:  
20  
21 fusion competence of parasitophorous vacuoles in Fc receptor-transfected fibroblasts.  
22  
23  
24 *Science* 1990;249:641–6.

## Figure Captions

Figure 1. TEM micrographs of CS/DNA and CS/DNA/ $\gamma$ -PGA complexes; schematic illustrations of their internal structures obtained by small angle X-ray scattering (SAXS), modified from our previous study [5]. CS: chitosan;  $\gamma$ -PGA: poly( $\gamma$ -glutamic acid).

Figure 2. (a) Kinetics of CS/DNA and CS/DNA/ $\gamma$ -PGA complexes mediated luciferase gene expressions ( $n = 3$ ,  $*P < 0.05$ ); (b) percentages of cellular uptake of FITC-labeled CS/DNA and CS/DNA/ $\gamma$ -PGA complexes ( $n = 3$ ,  $*P < 0.05$ ) and (c) their intracellular fluorescence intensities; (d) percentages of EGFP-expressing cells ( $n = 3$ ,  $*P < 0.05$ ). Lipofectamine: positive control; Control: the group without any treatment; CS: chitosan;  $\gamma$ -PGA: poly( $\gamma$ -glutamic acid).

Figure 3. Results obtained by the molecular dynamic simulations showing the presence of (a) intramolecular hydrogen bondings in  $\gamma$ -PGA (the N-terminal amine group in  $\gamma$ -PGA is hidden) and (b) intermolecular hydrogen bondings between chitosan and  $\gamma$ -PGA (the N-terminal amine group in  $\gamma$ -PGA is exposed).

Figure 4. Viability of the cells after being treated with distinct inhibitors, determined by the MTT assay ( $n = 5$ ). Control: the group without any inhibitor treatment.

Figure 5. Effects of inhibitors on the internalization of test complexes: (a) fluorescence intensities and (b) mean fluorescence intensities of intracellular uptake ( $n = 3$ ,  $*P < 0.05$ ); (c) EGFP intensities of cells pretreated with distinct inhibitors and then transfected with test complexes, determined by flow cytometry at 48 h after transfection ( $n = 3$ ,  $*P < 0.05$ ). Control: the group treated with test complexes only. CS: chitosan;  $\gamma$ -PGA: poly( $\gamma$ -glutamic acid).

Figure 6. TEM images showing the internalization pathways of test complexes. Arrowheads indicate test complexes; black arrows macropinocytosis; and while arrows caveolae-mediated pathway. CS: chitosan;  $\gamma$ -PGA: poly( $\gamma$ -glutamic acid).

Figure 7. (a) Images of the intracellular trafficking of test complexes observed by a confocal laser scanning microscope (scale bar: 8  $\mu\text{m}$ ); (b) quantitative analysis of Cy3-labeled test complexes colocalized with Lyotracker. CS: chitosan;  $\gamma$ -PGA: poly( $\gamma$ -glutamic acid).

Figure 8. Schematic illustrations of potential mechanisms of internalization of (a) CS/DNA complexes and (b) CS/DNA/ $\gamma$ -PGA complexes. CS: chitosan;  $\gamma$ -PGA: poly( $\gamma$ -glutamic acid).

Figure 1

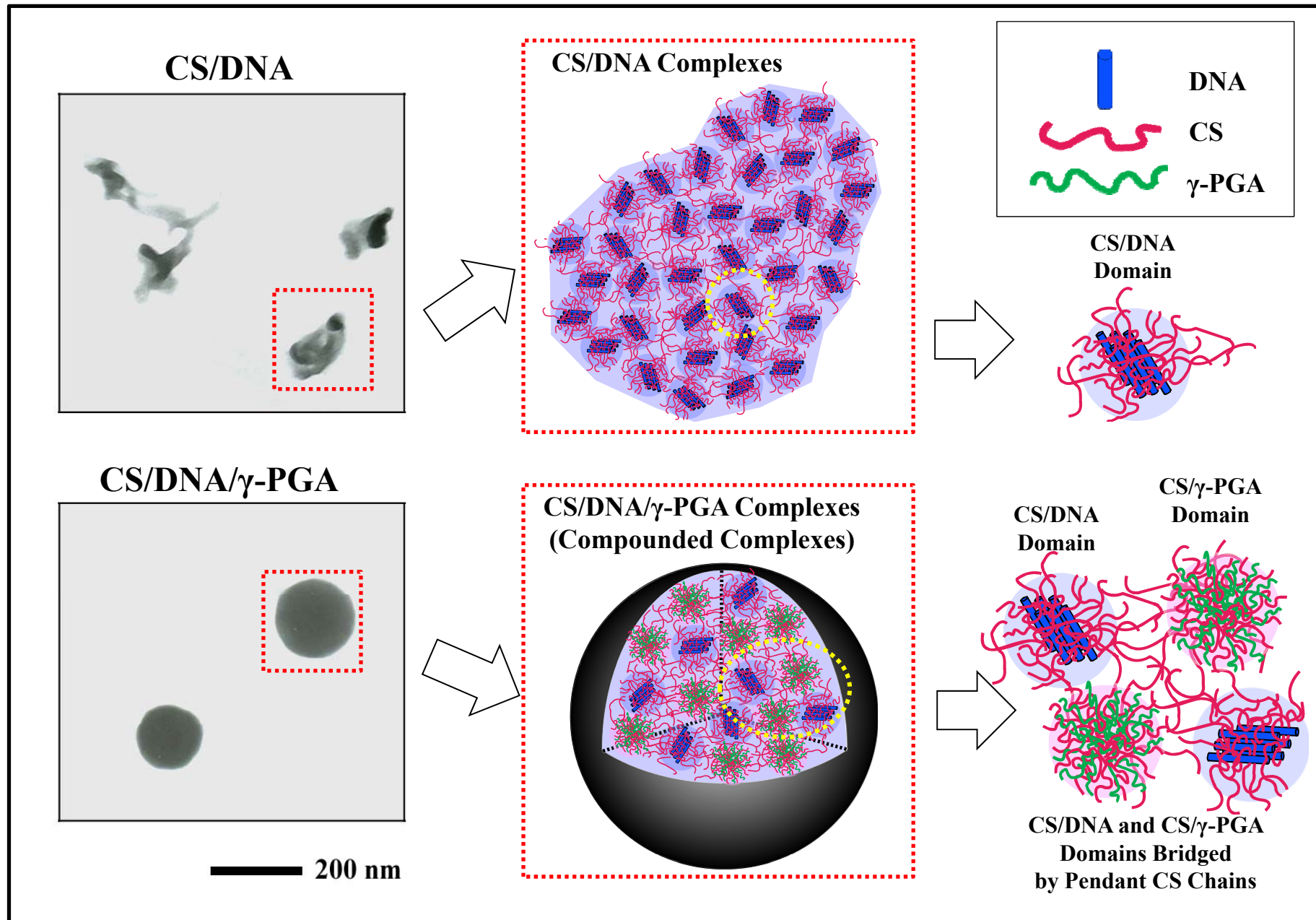


Figure 2

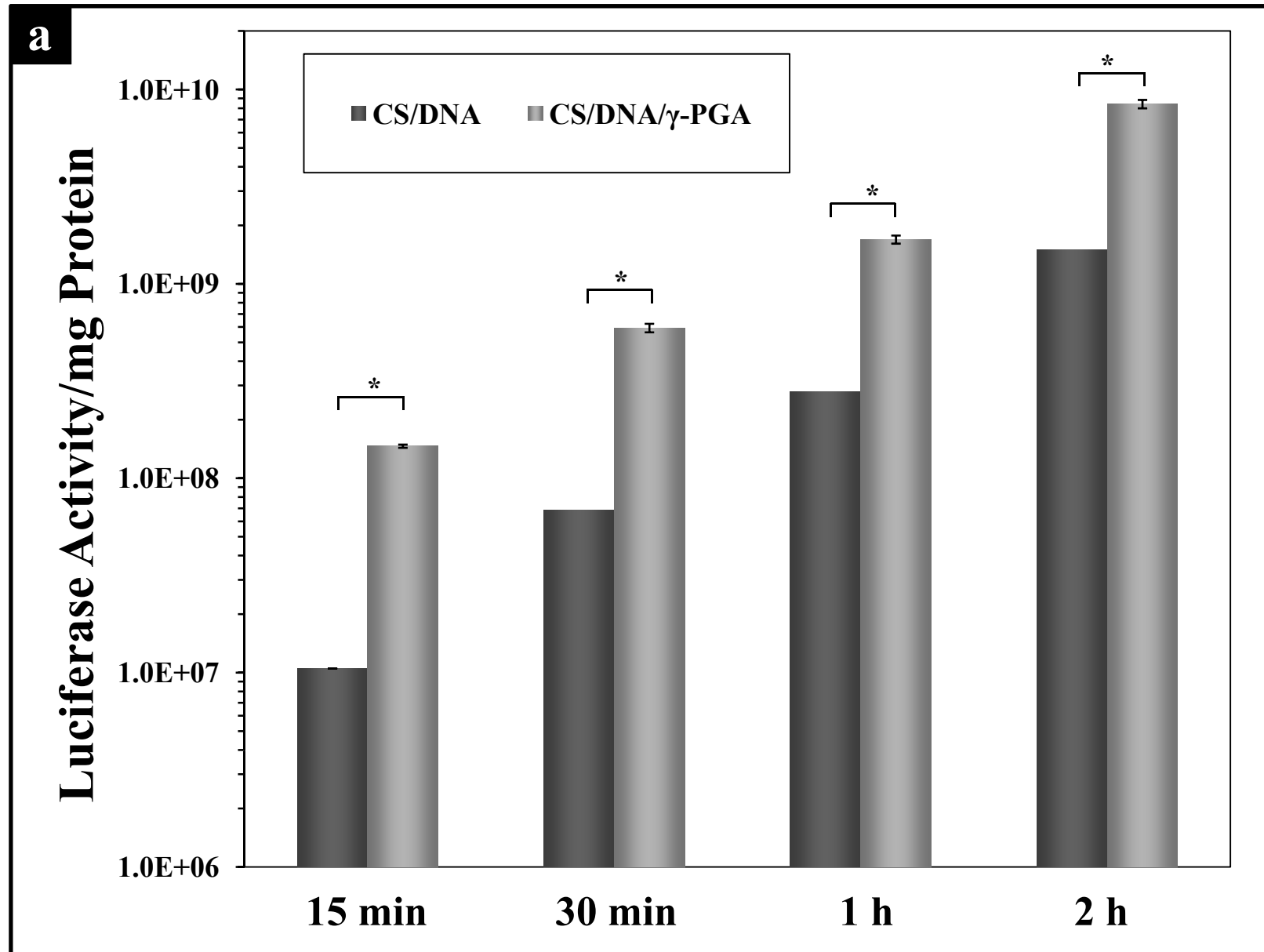


Figure 2

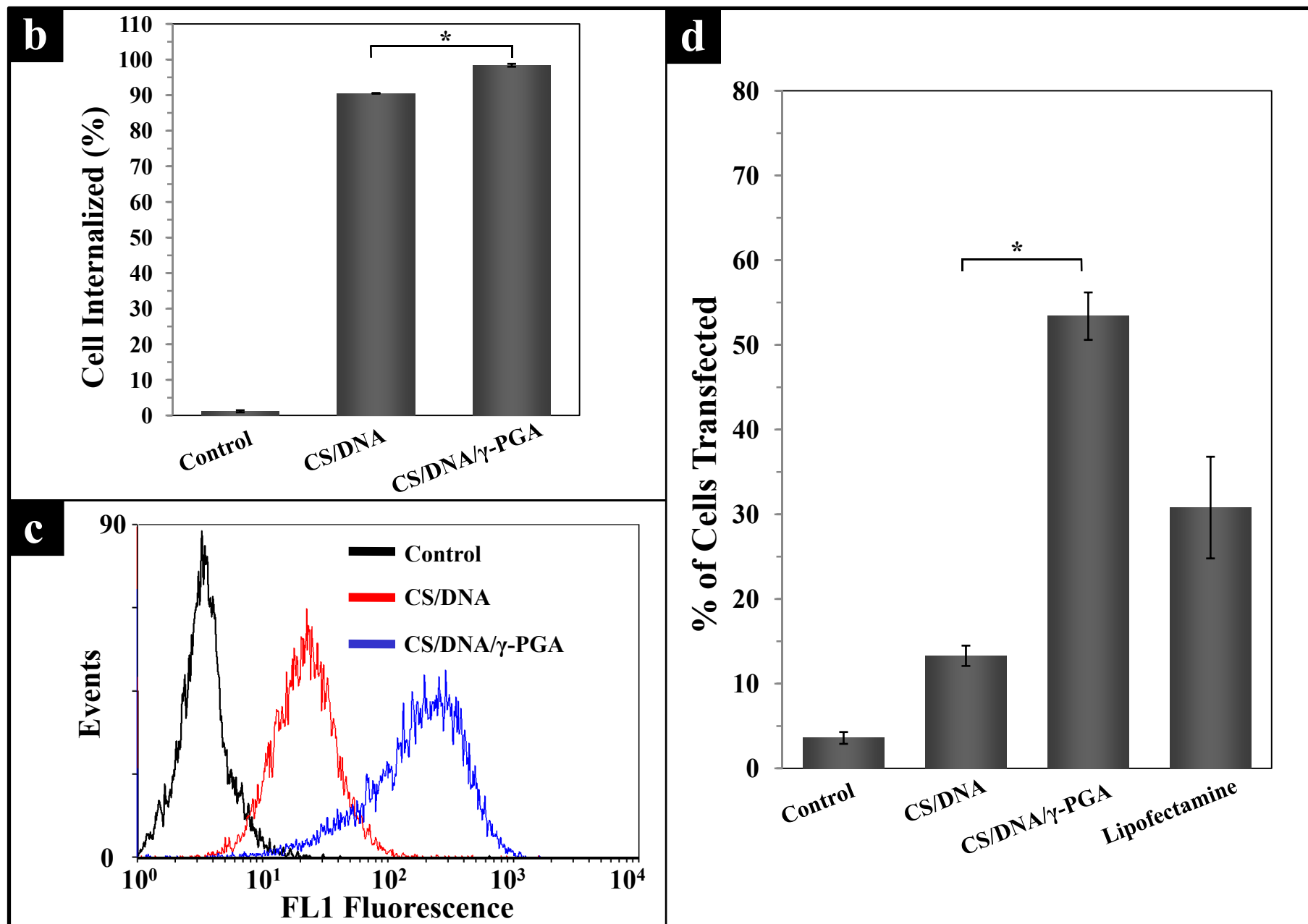


Figure 3

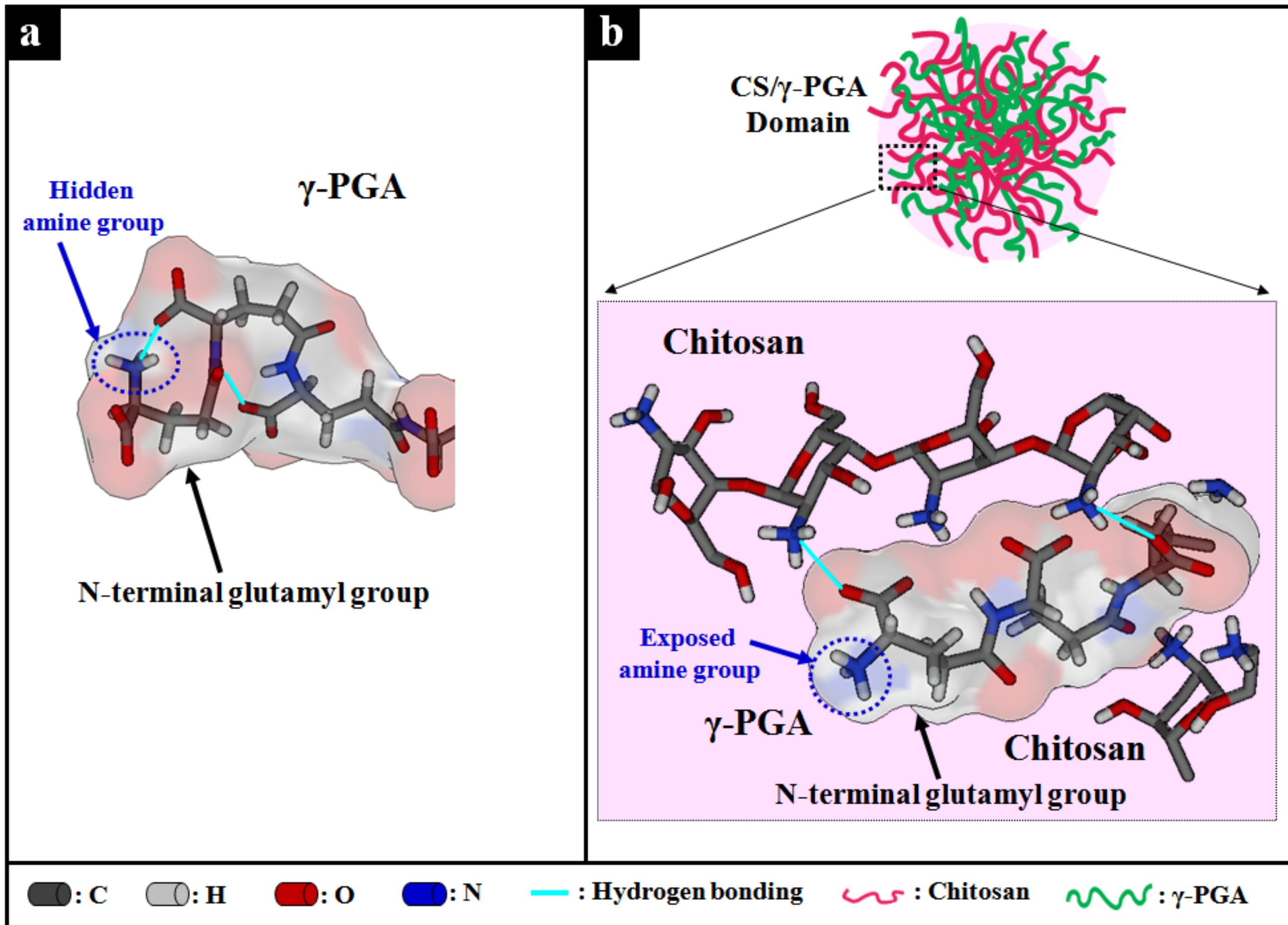


Figure 4

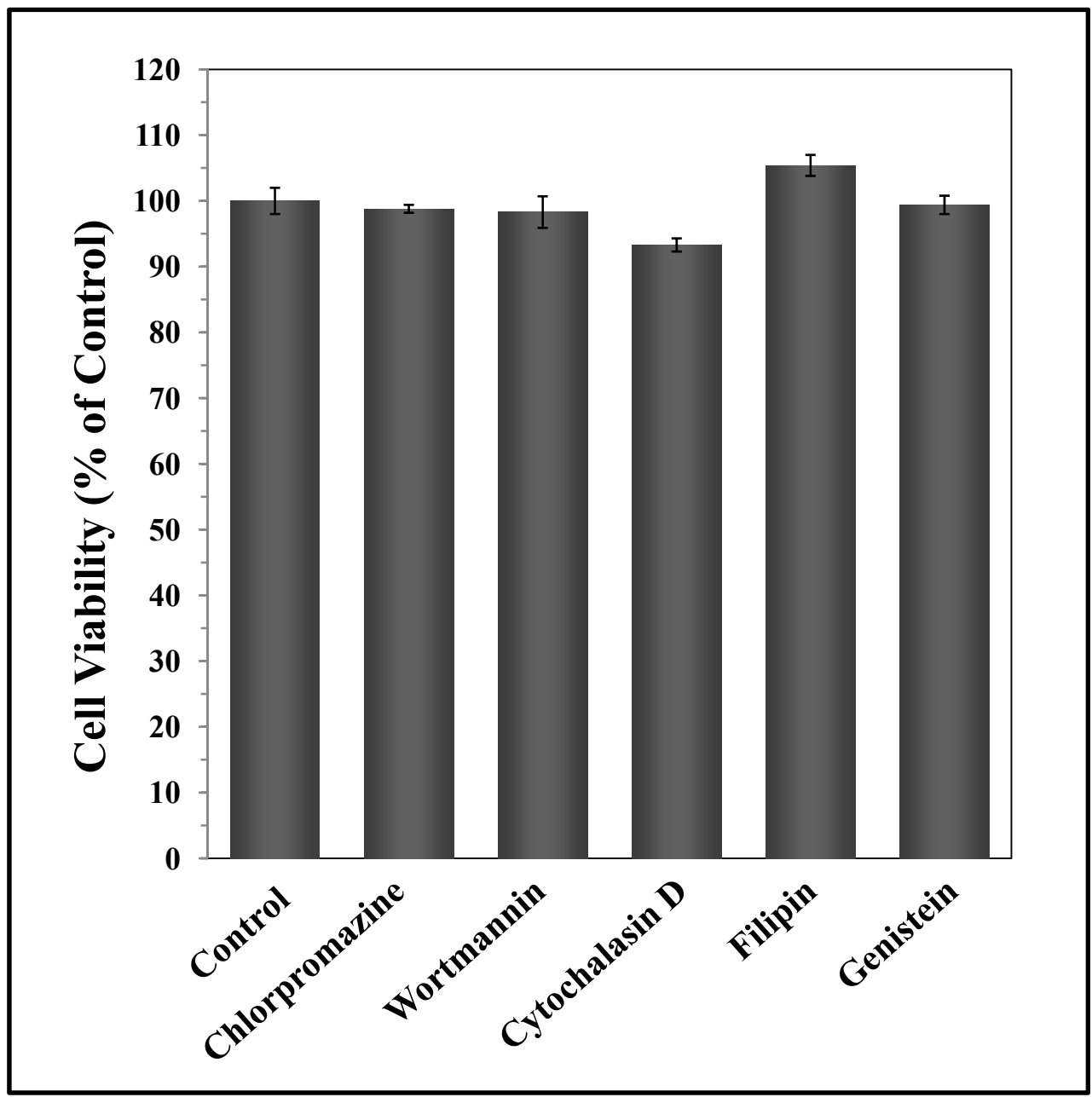


Figure 5

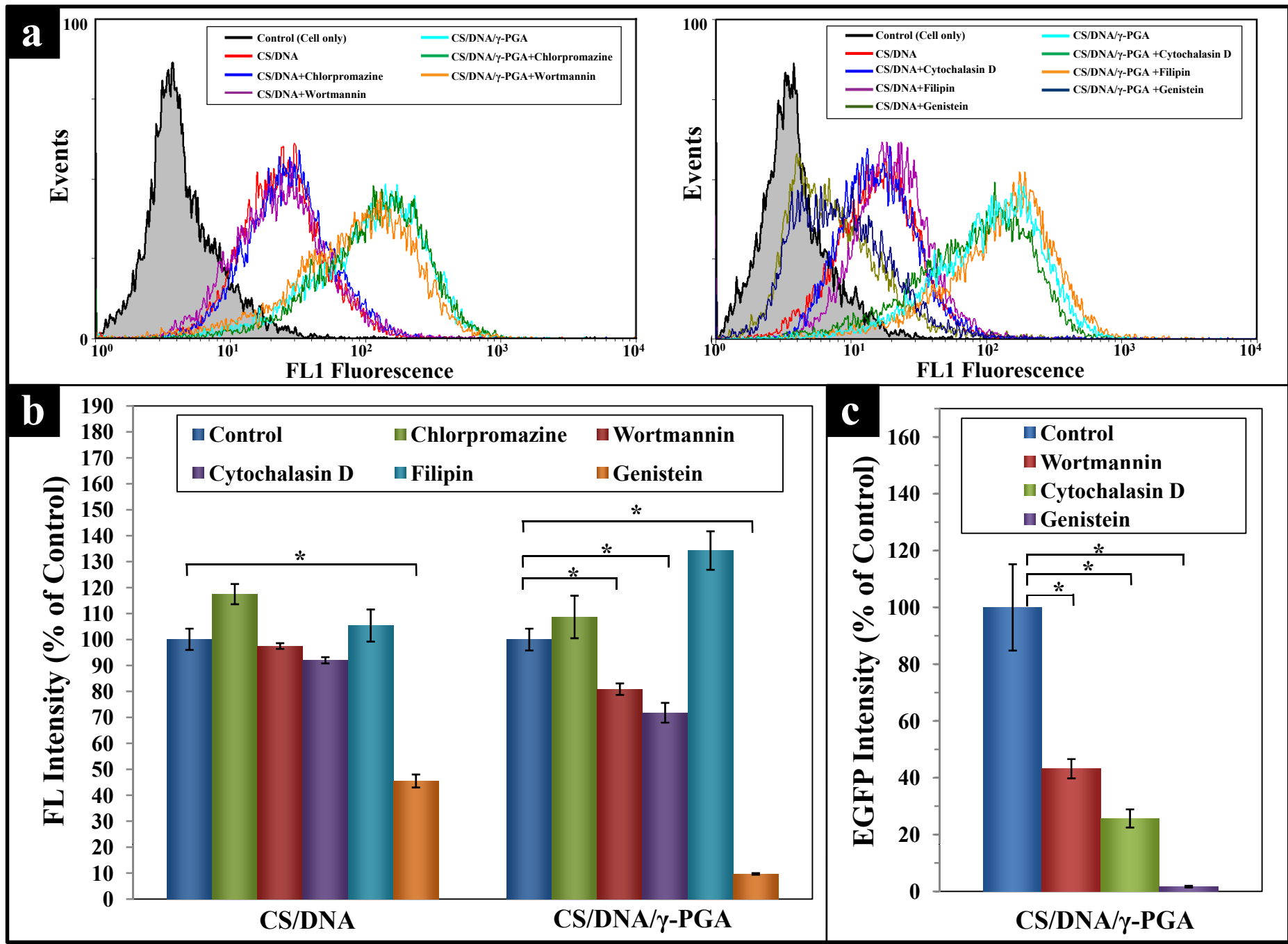
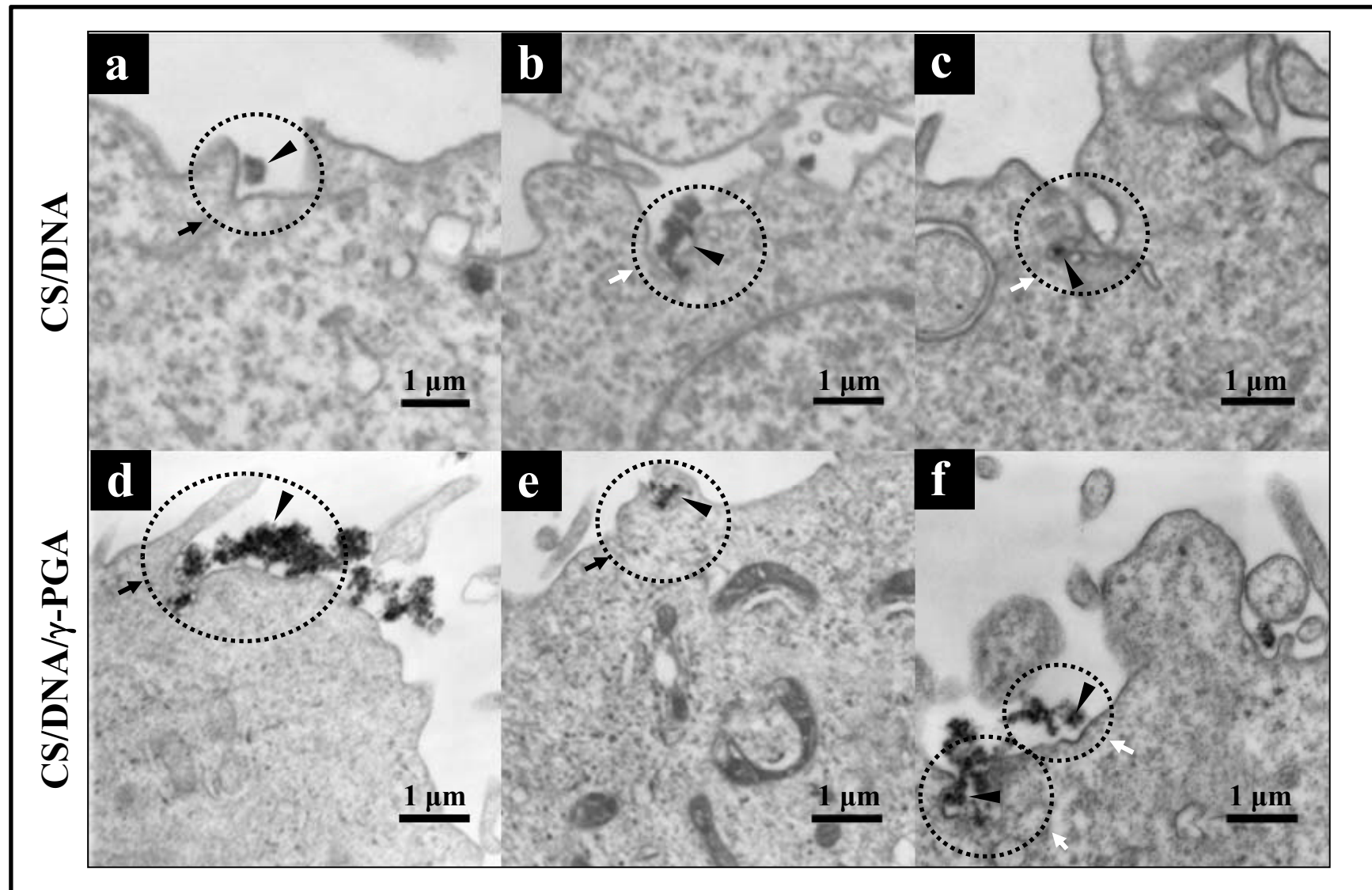


Figure 6



**Figure 7**

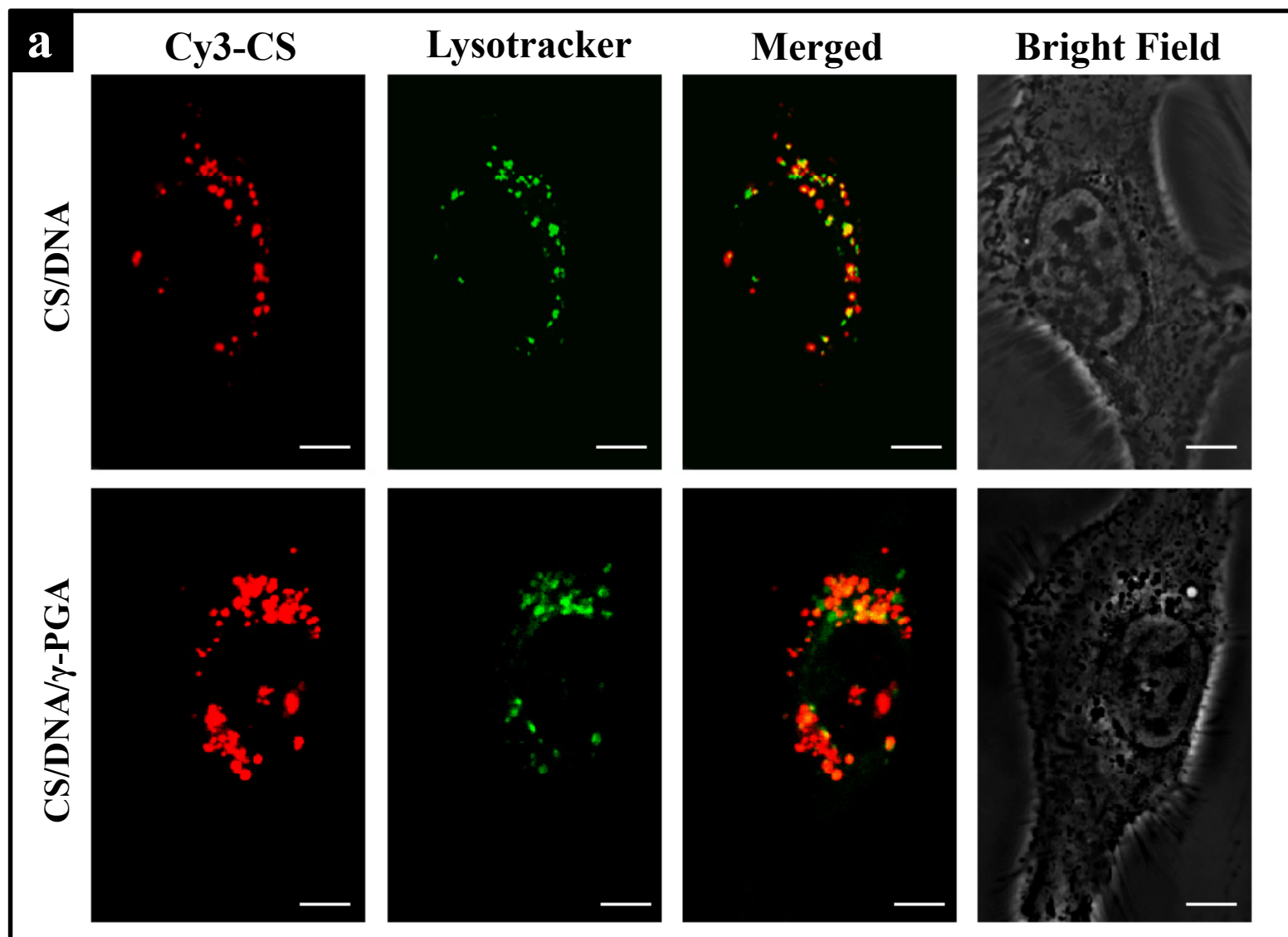


Figure 7

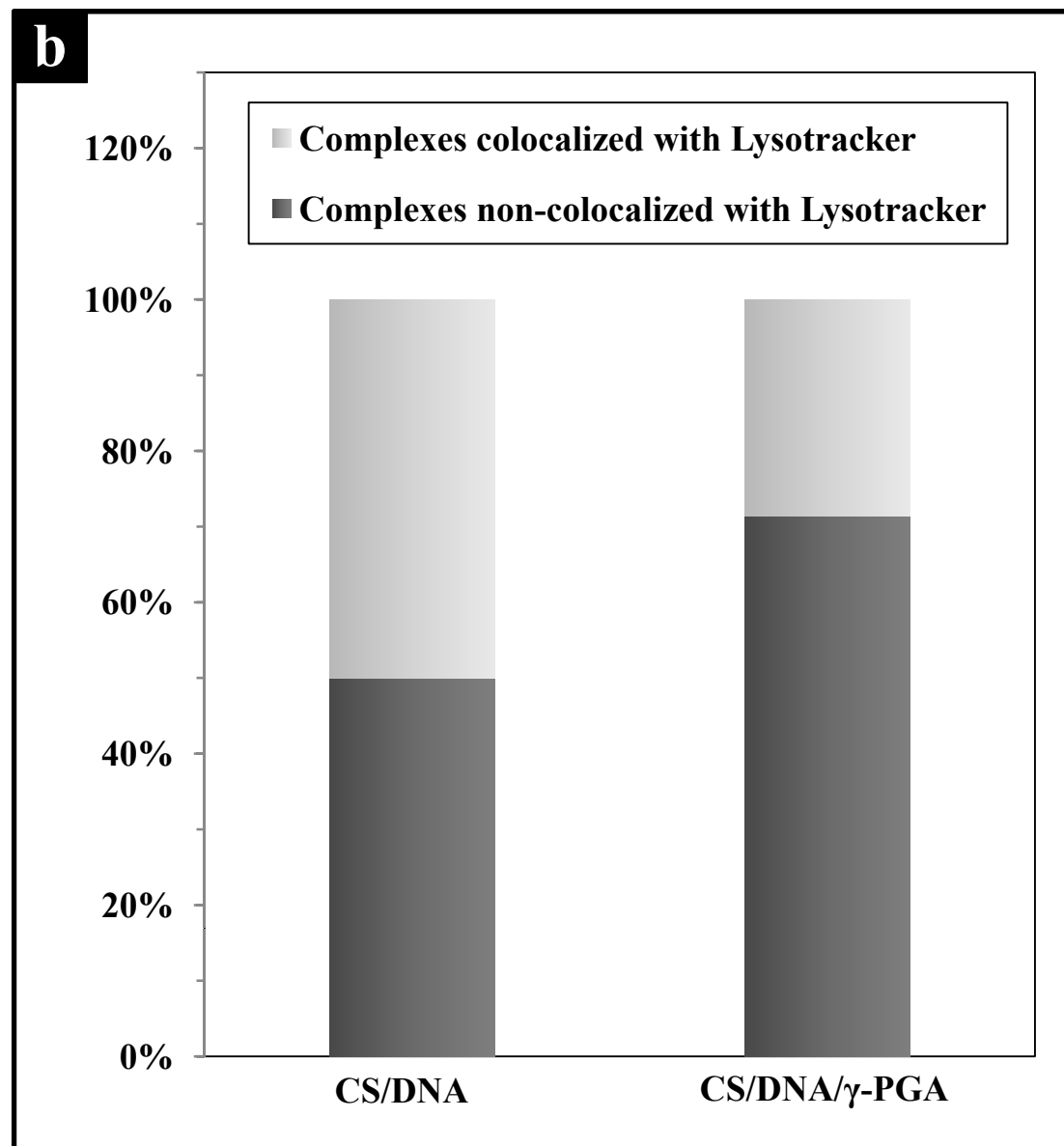


Figure 8

